



Evaluation of viral load and transcriptome changes in tracheal tissue of two hybrids of commercial broiler chickens infected with avian infectious bronchitis virus: a comparative study

Hamzeh Ghobadian Diali^{1,3} · Hossein Hosseini² · Mohammad Hossein Fallah Mehrabadi³ · Ramak Yahyaraeyat¹ · Arash Ghalyanchilangeroudi¹

Received: 12 April 2021 / Accepted: 19 October 2021 / Published online: 4 January 2022
© The Author(s), under exclusive licence to Springer-Verlag GmbH Austria, part of Springer Nature 2021

Abstract

Infectious bronchitis virus (IBV) is one of the major threats to the poultry industry, with significant economic consequences. Despite strict measures, the disease is difficult to control worldwide. Experimental evidence demonstrates that the severity of IBV is affected by the genetic background of the chicken, and the selection of appropriate breeds can increase production efficiency. Therefore, the aim of the present study was to assess the strength of the immune response to IBV in tracheal tissues of Ross 308 and Cobb 500 broiler chickens by evaluating transcriptome changes, focusing on immune responses and the viral load in tracheal tissues two days after IBV infection. We identified 899 and 1350 differentially expressed genes (DEGs) in the Cobb 500 and Ross 308 experimental groups compared to their respective control groups. Kyoto Encyclopedia of Genes and Genomes (KEGG) pathway enrichment analysis indicated the involvement of signaling pathways (Toll-like receptor [TLR], NOD-like receptor [NLR], and RIG-I-like receptor [RLR] signaling pathways). Interestingly, the RLR signaling pathway appears to be affected only in the Cobb hybrid. Furthermore, the viral loads in tracheal samples obtained from the Ross challenged group were significantly higher than those of the Cobb challenged group. The results of this study indicated that the host transcriptional response to IBV infection as well as the viral load can differ by hybrid. Furthermore, genes such as *TLR-3*, *ChIFN-α*, *MDA5*, *LGP2*, *IRF-7*, *NF-κB*, and *TRIM25* may interfere with IBV proliferation.

Introduction

With the ever-growing human population, there is a strong tendency for poultry to become the main protein source. Therefore, the poultry industry plays an important role in the food supply chain, and its economic significance cannot be ignored [1]. However, this industry faces various challenges, among which are infectious diseases, and viral diseases can cause huge economic losses to the industry worldwide [1, 2].

Infectious bronchitis virus (IBV) is one of the major threats to the industry and has significant economic consequences [1]. The causative agent of IBV is a positive-sense single-stranded RNA virus of the family *Coronaviridae* [3, 4].

The virus is known for its rapid reproduction with high mutation and recombination frequency, leading to geographically distinct strains [1, 5]. The virus enters through and replicates in the host's respiratory tract before respiratory signs start to appear within 24 to 48 hours of contact with the virus, and this is known as the incubation period [6, 7]. Some IBV strains may have tropism for other epithelial tissues (including the kidneys and oviduct), in which they cause infection and lesions [8–10]. The disease can be exacerbated when it coincides with secondary bacterial infections.

IBV affects chickens of all ages and can be transmitted rapidly across farms. Within three days of infection, clinical signs such as depression, poor weight gain, and appetite loss may appear. Furthermore, lesions caused by some strains in the oviduct markedly decrease egg quality and production [10, 11]. In addition, the mortality rate can

Handling Editor: Diego G. Diel.

✉ Arash Ghalyanchilangeroudi
ghalyana@ut.ac.ir

¹ Department of Microbiology and Immunology, Faculty of Veterinary Medicine, University of Tehran, Tehran, Iran

² Department of Clinical Sciences, Faculty of Veterinary Medicine, Islamic Azad University, Karaj Branch, Karaj, Iran

³ Department of Poultry Diseases, Razi Vaccine and Serum Research Institute, Agricultural Research, Education, and Extension (AEREO), Karaj, Iran

be as high as 83%, depending on the virus strain and health condition of the chickens [7, 12]. Considering the above facts, the poultry industry must adopt and implement policies and preemptive measures. Current preventive strategies are a hybrid of appropriate management practices, including temperature control mechanisms and advanced ventilation, and the use of attenuated and inactivated viral vaccines [13, 14]. Despite these measures, however, the disease has proven difficult to control worldwide due to the diversity of strains in different geographical regions and the absence of complete cross-protection between them [15]. Hence, developing preventive and therapeutic treatments is necessary to control the spread of the virus. Previous studies have suggested several ways to combat the disease. For instance, Jackwood et al. suggested that polyvalent vaccines containing circulating virus strains can be used for protection against the virus [5]. Moreover, recombinant vaccines containing S1 and N proteins have been reported to induce an immune response [16].

Although numerous studies have been conducted, the control of IBV continues to be a major challenge. To introduce more-effective vaccines and develop enhanced preventive measures, it is essential to understand defense mechanisms against poultry pathogens. Such understanding can provide invaluable insights into molecular pathogenesis in birds and various pathways involved in virus-host interactions. Recent advances in genomics, transcriptomics, proteomics, and metabolomics are now often incorporated into methodologies to analyze cellular and molecular interactions in biological systems [17].

The use of high-throughput techniques, such as microarray and next-generation sequencing (NGS), has gained momentum among researchers exploring the interactions between IBV and the host [3, 13, 14, 17–19]. These investigations have provided intriguing insights into how antiviral mechanisms in poultry function against the virus causing infectious bronchitis. To the best of our knowledge, no study has looked into transcriptome changes in the Ross 308 and Cobb 500 hybrids to investigate their antiviral responses to IBV.

Previous studies have revealed that the viral load can differ in different tissues of chickens infected with IBV [20, 21]. However, there is limited information about the evaluation of viral load in different hybrids of chickens infected with IBV. Additionally, the selection of appropriate genetic breeds has been shown to increase production efficiency [22]. Therefore, the aim of the present study was to evaluate transcriptome changes (by focusing on immune responses) and viral load in tracheal tissues of Ross 308 and Cobb 500 broiler chickens' infected with IBV using RNA sequencing (RNA-seq) and quantitative reverse transcription polymerase chain reaction (RT-qPCR) methods.

Materials and methods

Experimental design

In this randomized controlled experimental study, a total of 120 one-day-old female broiler chickens (Ross 308 and Cobb 500) were randomly divided into four experimental and control groups ($n = 30$): Cobb control (Cobb Con), Ross control (Ross Con), Cobb experimental (Cobb Exper), and Ross experimental (Ross Exper). The two hybrids were kept in separate rooms (60 chickens per room). The chickens were fed and watered separately in subgroups of 15. To avoid interference by maternal antibodies, an IDEXX IBV Ab ELISA Kit (USA) was used to measure anti-IBV antibody titers after three weeks according to the manufacturer's instructions. Chickens that were negative for anti-IBV antibodies were assigned to experimental subgroups, and chickens with positive antibody test results were excluded from the study. Immediately after this procedure, chickens in the experimental groups were challenged intranasally with 200 μ L of allantoic fluid containing 10^4 times the 50% egg infective dose (EID₅₀)/mL of the Var2-like (IS/1494/06-like) strain. Control groups received 0.2 mL of sterile phosphate-buffered saline (PBS) intranasally.

Virus strain and titration

The Iranian variant-2-like IBV strain IS/1494 was used in the study. The strain was isolated from an Iranian broiler farm in 2014 [23]. The EID₅₀ was calculated using the Reed–Muench method [24].

Sample collection and preparation

Two days after challenge, 10 chickens were randomly selected from each subgroup and euthanized according to the University of Tehran's ethical principles (i.e., inhalation of carbon dioxide followed by dislocation of their cervical vertebrae) under sterile conditions. Then, tracheal tissues were dissected and pooled for each subgroup and placed in sterile 5-mL tubes containing RNAlater solution (Thermo Fisher Scientific, Massachusetts, USA) to stabilize and protect RNA with immediate RNase inactivation. In addition, tissue was removed from individual chickens in each subgroup and placed in sterile 1.5-mL tubes containing RNAlater solution to measure the viral load and perform a RT-qPCR test to evaluate RNA-seq results. The pooled tracheal tissues were sent to BGI in China for paired-end sequencing using a HiSeq 2000 system and a

TruSeq SBS Kit v3-HS Illumina. All RNA extraction processes and quality control were performed by the company.

Total RNA from all pooled samples was extracted using the TRIzol method according to the instructions of the TRIzol Kit Manual (B518651-0100, Sangon Biotech, Shanghai, China). The RNA purity was determined based on spectroscopic measurements at 230, 260, and 280 nm using a spectrophotometer (IMPLEN, CA, USA), and the integrity of the RNA was assessed using a Bioanalyzer 2100 system and an RNA Nano Assay Kit (Agilent Technologies, Santa Clara, CA, USA). The RNA samples that passed the purity and integrity tests (i.e., RNAs with a minimum RNA integrity number (RIN) of 8.00, a A260/280 ratio of at least 1.80, and an A260/230 ratio of at least 2.00) were used for transcriptome sequencing using an Illumina HiSeq 2000 platform.

Transcriptome analysis

About 31 million paired-end raw reads for each sample with a length of 90–100 base pairs (bp) were generated from RNA-seq libraries in FASTQ format. Before read alignment, the FastQC tool (<https://www.bioinformatics.babraham.ac.uk/projects/fastqc>) was used for quality control of raw reads, and the reads were pre-filtered to remove probable contaminants. Quality trimming increased the number of good reads and abundance measurement accuracy. Adapter sequences and low-quality nucleotide calls in the raw data were removed using BBDuk 38.87 (BBtools, California, USA). For adapter sequence trimming, we used the following parameters: $ktrim = r$, $k = 23$, $mink = 11$, and $hdist = 1$. For nucleotide trimming, the nucleotide calls with a quality score of 20 or higher were considered high-quality reads. We defined r and l (right and left side trimming) for the “--qtrim = rl” parameter and passed quality score 20 for quality trimming thresholds to the “--trimq” parameter.

After trimming, to identify reads originating from the chicken genome, we aligned clean reads to the reference genome sequence GRCg6a (GCA_000002315.5) using Spliced Transcripts Alignment to a Reference (STAR) with default settings.

The reference genome sequence and annotation files were obtained from the Ensembl database (<https://asia.ensembl.org/info/data/ftp/index.html>), and genome indexing was done using the “--runMode genomeGenerate” option in the STAR software package 2.7. [25]. After alignment, several files were created, and the “ReadsPerGene.out.tab” file (a tab-delimited text file with read count per gene used for expression analysis) was the main file used for subsequent analysis to identify differentially expressed genes (DEGs).

Identification of DEGs

DEGs were identified using the edgeR software package version 3.28.1. Here, only genes with a log fold change ≥ 1 or ≥ -1 ($P < 0.05$) were identified as DEGs. To create the figure showing DEGs, we constructed a heat map using the R software package (pheatmap) version 1.0.12 (<https://cloud.r-project.org/web/packages/pheatmap>). An MD plot was made to show the log-fold change of DEGs in the experimental groups compared to the controls, and the average abundance of each gene was determined using the R software package (plotMD).

Functional annotation analysis

To identify biological functions related to DEGs, the Kyoto Encyclopedia of Genes and Genomes (KEGG) pathways and Gene Ontology (GO) terms (cellular component, molecular function, and biological process) were investigated using the DAVID database (version 6.8) (<https://david.ncifcrf.gov/>) [26]. GO terms and KEGG pathways with a P -value < 0.05 were considered to exhibit statistically significant enrichment.

Validation of RNA-seq results and calculation of viral load using RT-qPCR

An RT-qPCR assay was used to evaluate and confirm the results obtained using the RNA-seq method and to calculate the viral load, in individual Cobb and Ross chickens in the study groups.

Total RNA was extracted from individual samples taken from each subgroup using a SinaPure RNA Kit (SinaClon, Iran) and treated with DNase I. The purity of the total RNA was determined using spectroscopic measurements at 230, 260, and 280 nm. The RNA integrity was evaluated by electrophoresis on a 1% agarose gel after staining with ethidium bromide and visualization under UV light (for more details, see Supplementary File 1). RNA samples with an OD260/280 ratio of 1.9–2.2 and an OD260/230 ratio greater than 2 and with high integrity (i.e., RNAs with clearly visible bands of 18S and 28S ribosomal RNA) were used for cDNA synthesis.

cDNA synthesis was performed using a RevertAid First Strand cDNA Synthesis Kit (Fermentas, Canada) as follows: a mixture of 2 μ g of total RNA (7 μ L RNA), 1 μ L of random hexamer primer, and 4 μ L of DEPC-treated water was heated at 65 °C for 10 min and cooled on ice. Then, 4 μ L of 5X reaction buffer, 1 μ L of Ribolock Rnase inhibitor (20 U/ μ L), 2 μ L of 10 mM dNTP mix, and 1 μ L

Table 1 Primers used in RT-qPCR for the Cobb chickens

Gene	Forward primer (5'-3')	Exon Nucleotide position	Reverse primer (5'-3')	Exon Nucleotide position	Size (bp)	Efficiency (%)	Slope	Gene expression status
<i>TLR7</i>	CAGTGGTTG CTGCTGTTG TC	Exon 1 43-62	GCATTTGAC GTCCTTGCA TGA	Exon 2 221-201	179	105	3.20	Up
<i>NRROS</i>	GAGAGCTGC TGCTGAGAT GGAG	Exon 2 7565-7586	GCTCAACCA TTTCCTTT GCAGTC	Exon 3 7727-7704	163	104	3.22	Up
<i>THEMIS</i>	TAAGTGCAG AAGCCGGAC TG	Exon 3 831-850	CGTCTCCA AAGACAGTG GC	Exon 4 1069-1050	239	103	3.23	Up
<i>BEST1</i>	TCGTTCCCT GGATCAACC TTTG	Exon 8 3957-3978	TCCGGGAAG AGGATCTGG AG	Exon 9 4128-4109	172	99	3.33	Up
<i>MUC13</i>	AGTCTCAGT TGTTTCAGT AAG	Exon 22 1472-1492	CTCATAAGG GTTGTTTGG CT	Exon 23 1643-1624	172	97	3.38	Up
<i>DHX58 (LGP2)</i>	AGCTCCACG GGTACCAAC	Exon 1 5-22	TTCTCCAAG TGCTGCTGC	Exon 2 197-180	193	99	3.33	Up
<i>IFIH1 (MDA5)</i>	CAAGAACAG AAAGCAGGC	Exon 7 1516- 1533	CCTTCTTTTGTC ATCTGCA	Exon 8 1759- 1741	244	96	3.41	Up
<i>MHM2</i>	AATCCCTCC TGCCACAGC	Exon 2 95-112	ACTTGGGGC ACGGTGGT	Exon 2 311-295	217	96	3.41	Down
<i>LUZP2</i>	GATGAATTG GAAAAGGCAG	Exon 8 1103-1121	CTTTCGAGC CCTTTGTAG	Exon 9 1271-1254	169	99	3.25	Down
<i>PLS1</i>	ATCTACGGA AGGGACACAG	Exon 5 460-478	GAATGCCAT CTGCAAGGGA	Exon 6 617-599	158	106	3.18	Down
<i>RALY</i>	TAGATCGGC TGCCATTG	Exon 6 653-669	CTGTGGACT GTTTCTGTTC	Exon 7 807-789	155	99	3.34	Down
<i>SBK2</i>	TATGAACCA GCAATGCAC	Exon 3 595-612	GTGTAAGCC CAAAATCAGT	Exon 6 808-790	214	103	3.24	Down
<i>GAPDH</i>	CTGCCGTCT GGAGAAACC	Exon 8 789-806	CCAGCACCC GCATCAAAG	Exon 10 950-933	162	99	3.33	Reference

of RevertAid M-MuLV Reverse Transcriptase (200 U/ μ L) were added to the solution to a final volume of 20 μ L.

To validate RNA-seq results, 22 genes were selected randomly from each up- and downregulated DEG from both hybrids. All RT-qPCR primers were designed using Primer-BLAST [27], and their sequences are shown in Tables 1 and 2. For RT-qPCR, the 20- μ L reaction mixture contained 2 μ L of cDNA, 10 μ L of SYBR Premix (SinaClon, Iran), 0.4 μ L of forward and 0.4 μ L of reverse primers at a final concentration of 10 μ M, and 7.2 μ L of RNase-free water. The reaction condition were as follows: 95 $^{\circ}$ C for 5 min, followed by 40 cycles of 95 $^{\circ}$ C for 15 s, 56 $^{\circ}$ C (*CDRT1*, *NRROS*, *MHM2*, *TLR7*, *THEMIS*, *BEST1*), 55 $^{\circ}$ C (*LGP2*, *GAPDH*, *PLS1*, *TBX21*, *TLR1B*), 51 $^{\circ}$ C (*FAM81A*, *AHR2*, *MUC13*, *MYH15*, *RALY*, *FCN2*, *SBK2*), or 48 $^{\circ}$ C (*MDA5*, *LUZP2*, *ARHGAP15*, *GPR171*, *ADAP2*) for 20 s, and 72 $^{\circ}$ C for 15 s using a Corbett Life Science Rotor-Gene 6000 Cycler (USA). The fold changes in expression

were calculated using the $2^{-\Delta\Delta CT}$ method [28]. All samples used for RT-qPCR were analyzed in triplicate.

To calculate the viral load, cDNAs from individual tracheal samples in each subgroup were used to amplify a conserved sequence of the IBV genome within the 5' untranslated region (UTR) by real-time PCR. The forward primer 5'-GCTTTTGAGCCTAGCGTT-3', located at nucleotide position 391–408 of the genome sequence of IBV strain M41, the reverse primer 5'-GCCATGTTGTCAGTGTCTATTG-3', located at nucleotide position 512–533, and a TaqMan dual-labeled probe (IBV5'G probe 5'-FAMCAC CACCAGAACCTGTACCTC-BHQ1-3') located at nucleotide position 473–494 were designed to amplify and detect a 143-bp fragment of the 5'-UTR [20, 29]. The 20- μ L reaction mixture contained 2 μ L of 10x PCR buffer (Sinaclon), 1 μ L of dNTP mix (Sinaclon), 0.8 μ L of 50 mM MgCl₂ (Sinaclon), 0.2 μ L of CinnaGen Taq DNA polymerase (Sinaclon), 5 μ L of template cDNA, 0.4 μ L of forward and 0.4 μ L of

Table 2 Primers used in RT-qPCR for the Ross chickens

Gene	Forward primer (5'-3')	Exon Nucleotide position	Reverse primer (5'-3')	Exon Nucleotide position	Size (bp)	Efficiency (%)	Slope	Gene expression status
<i>TBX21</i>	CCACAAACATCA GACCGAG	Exon 1 598-616	CATTTGCCGCC TGGTA	Exon 2 759-743	162	99	3.34	Up
<i>TLR1B</i>	TGCAAGTACCCA GAAGAC	Exon 5 1352-1369	AGCATCCGCACG TACCA	Exon 5 1524-1508	173	99	3.25	Up
<i>GPR171</i>	ACTACTTGATCT TTCTTACG	Exon 2 223-242	CTTGGCAGTGGA ATATCT	Exon 2 426-409	204	104	3.22	Up
<i>ADAP2</i>	GGCTTCTTACAA ACTTGG	Exon 2 144-161	CTCTAATCCATT GTTCTCT	Exon 4 382-364	239	104	3.22	Up
<i>ARHGAP15</i>	CTGTTCCCATAC TGCTTC	Exon 14 1107-1124	GACATAAGATTC ACGGATTC	Exon 16 1288-1269	182	99	3.33	Up
<i>FAM81A</i>	GAACAGGAACAC GAGAGG	Exon 4 1623-1640	GTCTGTTGTGTT TCATGTGC	Exon 5 1810-1791	188	99	3.33	Down
<i>AHR2</i>	CGCTGCTTGCTG GATAA	Exon 6 923-939	GAAAGGCTG AAAGGGAGT	Exon 7 1075-1058	153	96	3.41	Down
<i>MYH15</i>	GTACAACCTGAG GAAGCG	Exon 3 526-543	GGAGAAGATGTG AGGAGG	Exon 4 688-671	163	103	3.23	Down
<i>CDRT1</i>	CAGGCAGAGCAG CAAGAGC	Exon 12 3790-3808	TGGAGCGGACAA AGGATGGC	Exon 13 3964-3945	175	103	3.23	Down
<i>FCN2</i>	TTTAGGAGAGTC TGAGAAATAC	Exon 8 2603-2624	AGTACATGCCAT TGAGGTTA	Exon 9 2805-2786	203	99	3.34	Down
<i>GAPDH</i>	CTGCCGTCTGGA GAAACC	Exon 8 789-806	CCAGCACCCGCA TCAAAG	Exon 10 950-933	162	99	3.33	Reference

reverse primer at a concentration of 20 μ m, 0.4 μ L of probe at a concentration of 20 μ m, and 9.8 μ L of RNase-free water. The reaction was performed using a Corbett Life Science Rotor-Gene 6000 Cycler. The PCR cycling parameters were 95 °C for 3 min, followed by then 44 cycles of 95 °C for 15 s, 60 °C for 30 s, and 72 °C for 20 s [20].

Data analysis

An independent two-sample *t*-test was used to compare the expression levels of DEGs and the viral loads between the study groups. All analyses were performed at a significance

level of 5%. Stata 14 (StataCorp, College Station, Texas, USA) was used for data analysis.

Results

Gene expression profile

The number of raw, trimmed, and mapped reads and the mapping efficiency for each sample are presented in Table 3. After filtering, the overall QC percentage of high-quality clean data was above 95%. An average of 60 million trimmed reads per sample were mapped to the reference with

Table 3 Proportion analysis of reads (raw, trimmed, and mapped) in the Cobb 500 and Ross308 hybrids

Sample name	Number of raw reads	Number of reads after trimming	Number of unique trimmed reads mapped to the reference genome
Cobb control-1	30,134,660	30,043,797 (99.69%)	25,432,421 (84.65%)
Cobb control-2	30,211,444	30,099,286 (99.62%)	25,945,584 (86.20%)
Cobb experiment-1	30,263,219	30,173,169 (99.70%)	24,548,890 (81.36%)
Cobb experiment-2	30,289,132	30,143,554 (99.51%)	26,827,762 (89.00%)
Ross control-1	30,512,057	30,442,382 (99.77%)	24,658,329 (81.00%)
Ross control-2	30,571,989	30,478,334 (99.69%)	25,906,583 (85.00%)
Ross experiment-1	30,393,984	30,312,686 (99.73%)	24,522,962 (80.90%)
Ross experiment-2	30,432,996	30,338,676 (99.69%)	25,302,455 (83.40%)

a mapping efficiency of 80.90%–89.00%. Of the annotated genes in the chicken genome, 899 in Cobb 500 chickens (723 upregulated and 176 downregulated [Supplementary File 2]) and 1350 in Ross 308 chickens (650 upregulated and 700 downregulated [Supplementary File 3]) were identified as DEGs when comparing the experimental groups to their respective control groups (Fig. 1). MD plot, MDS plot, and a heat map of DEGs for each hybrid is presented in Figure 2. A Venn diagram showing the overlap of DEGs between the two hybrids is presented in Figure 3.

Functional annotation of DEGs

A functional annotation analysis was performed to determine functional categories of the DEGs. The 10 most enriched GO terms in each category (biological processes, molecular function, and cellular components) related to upregulated genes in both hybrids are listed in Tables 4, 5, 6. Additionally, the five most enriched GO terms in each category related to downregulated genes in both hybrids are shown in Figure 4.

KEGG pathway analysis

KEGG pathway analysis was performed to investigate the biological functions of the DEGs [30]. The KEGG pathways were significantly enriched in the subsets of up- and downregulated genes in each hybrid. The KEGG pathway enrichment analysis showed that the upregulated genes were mainly involved in signaling pathways (Toll-like receptor [TLR] signaling, JAK-STAT signaling, NOD-like receptor [NLR] signaling, and RIG-I-like receptor [RLR] signaling pathways) (Table 7). Interestingly, the RLR signaling pathway (including *IFIH1* [also known as *MDA5*] and *DHX58* [also known as *LGP2*]) was affected only in the Cobb 500

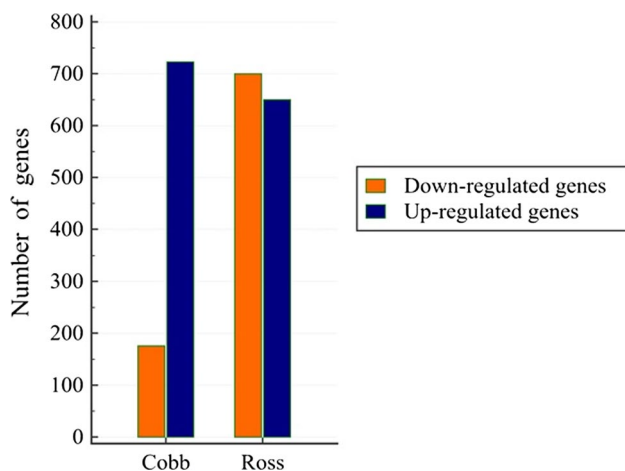


Fig. 1 Comparison of DEGs in the tracheal tissue of the Cobb 500 and the Ross 308 hybrids two days after infection with IBV

hybrid. The KEGG pathway enrichment analysis results for the downregulated genes are presented in Figure 4.

Validation of RNA-seq results by RT-qPCR

qPCR analysis confirmed that the selected genes were differentially expressed between the experimental groups (Fig. 5). Furthermore, no significant difference in the expression levels of the selected DEGs was observed between the RNA-seq results and the RT-qPCR results, indicating that the RNA-seq results were indeed reliable (Tables 8 and 9). In addition, we used agarose gel electrophoresis to confirm the specificity of the real-time PCR assay (Fig. 6), and the identity of the PCR products was confirmed by Sanger sequencing.

Determination of the viral load by RT-qPCR

The viral load in tracheal tissues was measured two days after infection for all study groups. The virus was detected in all samples from the infected groups, and all samples from the control groups were negative. Statistical analysis showed that two days after infection, the mean viral load in the tracheal samples of the Ross challenged group was significantly higher than in the Cobb challenged group (P -value < 0.0001) (Fig. 7).

Discussion

The respiratory system is the main entry point for respiratory pathogens, including IBV. Therefore, examining changes in the transcriptome and viral load in infected respiratory tissues can provide vital details about virus-host interactions. To the best of our knowledge, this is the first study to evaluate transcriptome changes (focusing on immune responses) and viral load in tracheal tissues of Ross 308 and Cobb 500 broiler chickens infected with IBV using RNA-seq and RT-qPCR methods two days after infection.

We identified 899 genes in the Cobb 500 experimental group and 1350 genes in the Ross 308 experimental group that were expressed at different levels from those of the corresponding control group, and these results were confirmed using RT-qPCR. However, the calculated fold-change values were different. This may be due to differences in how the fold change was calculated from the RNA-seq and RT-qPCR data. Identification of DEGs provides potentially important information about the host's responses to IBV infection.

Our analysis identified three signaling pathways, all of which are associated with innate immune responses involving pattern-recognition receptors (PRRs), including the TLR, NLR receptor, and RLR signaling pathways. Interestingly, the RLR signaling pathway was not found to respond to IBV infection in the Ross 308 hybrid. Furthermore, at two

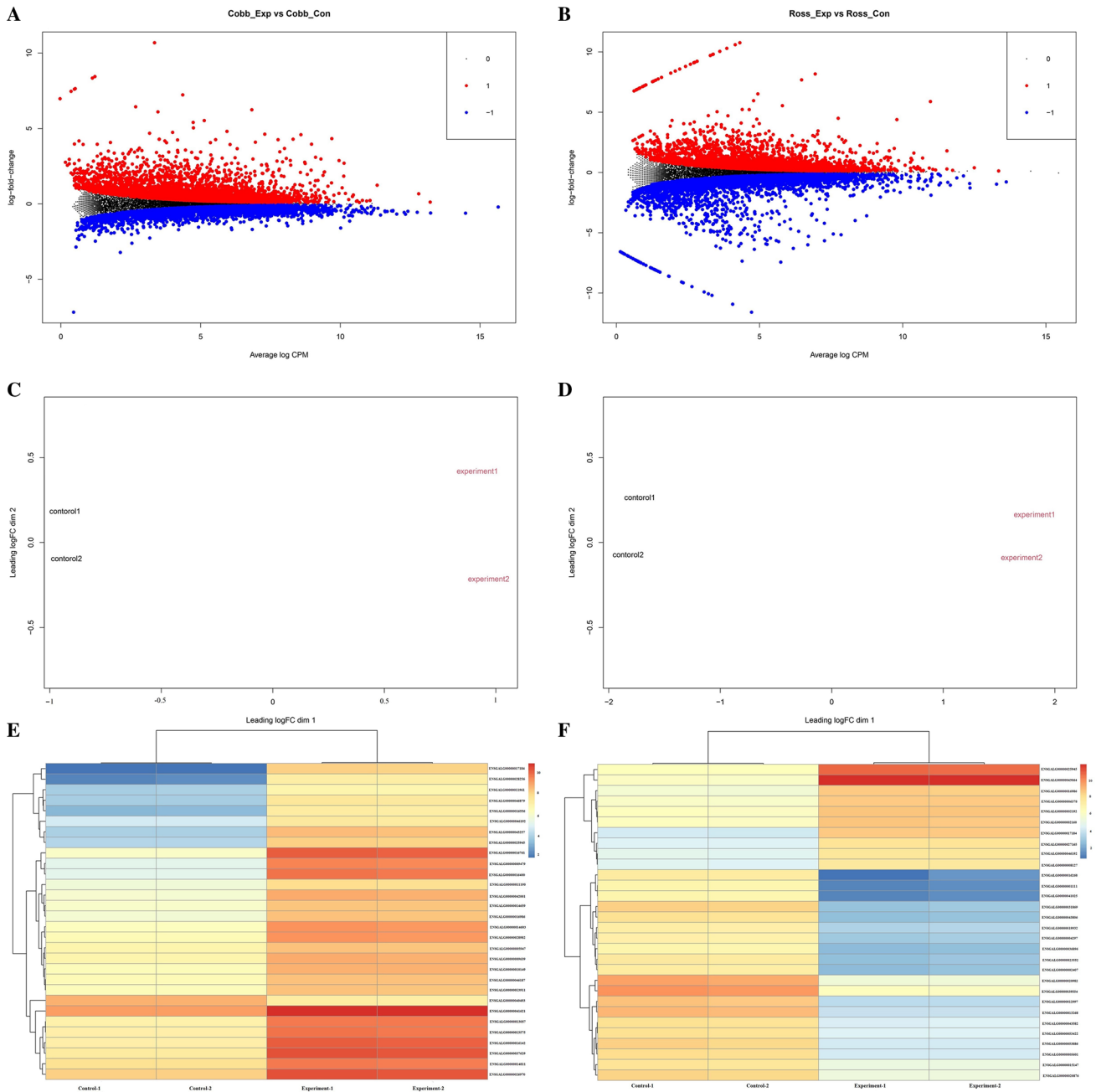


Fig. 2 MD-plot, MDS-plot, and heat map of DEGs of Cobb 500 (A, C, and E) and Ross 308 (B, D, and F). Significantly up- and downregulated genes are indicated in red and blue, respectively, in MD-plot.

Fig. 3 Venn diagram showing the overlap of upregulated genes (A) and downregulated genes (B) in Cobb 500 and Ross 308 chickens

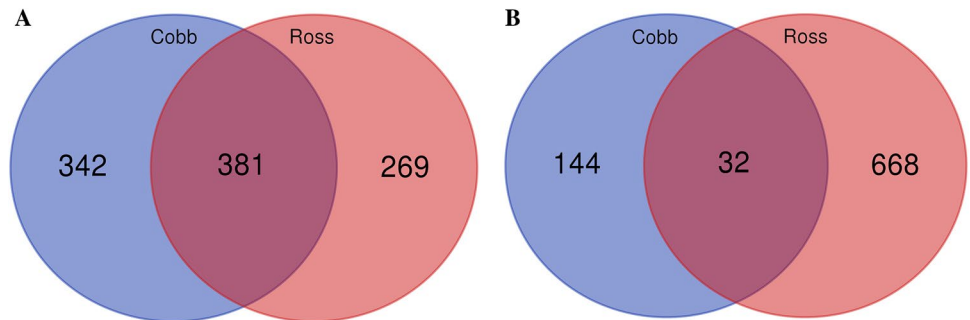


Table 4 Comparison of the top 10 GO anthology (Biological Process) results for upregulated differentially expressed genes in the Cobb 500 and Ross 308 hybrids

Biological Process in the Cobb 500 breed	Count	-Log <i>P</i> -value
Immune system process	186	65.43
Immune response	131	62.64
Defense response	109	37.60
Regulation of immune response	70	32.74
Regulation of immune system process	100	32.17
Positive regulation of immune system process	78	31.68
Leukocyte activation	74	28.85
Activation of immune response	50	27.82
Innate immune response	60	27.82
Positive regulation of immune response	58	27.77
Biological Process in the Ross 308 breed	Count	-Log <i>P</i> -value
Immune system process	160	51.89
Immune response	109	47.12
Positive regulation of immune system process	72	29.52
Regulation of immune system process	90	28.46
Regulation of immune response	61	27.16
Leukocyte activation	67	25.85
Defense response	85	23.96
Cell activation	70	23.28
Positive regulation of immune response	50	22.59
Lymphocyte activation	58	21.74

Table 5 Comparison of the top 10 GO anthology (Cellular Component) results for upregulated differentially expressed genes in the Cobb 500 and Ross 308 hybrids

Cellular Component in the Cobb 500 breed	Count	-Log <i>P</i> -value
Plasma membrane	176	13.21
Plasma membrane part	117	13.14
Cell periphery	179	12.96
Membrane part	253	11.05
Membrane	311	10.06
Integral component of membrane	213	8.80
Intrinsic component of membrane	214	8.49
Side of membrane	31	7.52
Intrinsic component of plasma membrane	68	6.55
Integral component of plasma membrane	65	6.10
Cellular Component in the Ross 308 breed	Count	-Log <i>P</i> -value
Plasma membrane	160	13.12
Plasma membrane part	107	13.00
Cell periphery	162	12.64
Side of membrane	34	10.72
Membrane part	217	8.00
T cell receptor complex	8	7.09
Membrane	267	6.89
External side of plasma membrane	18	6.57
MHC protein complex	7	5.92
Extrinsic component of cytoplasmic side of plasma membrane	14	5.37

Table 6 Comparison of the top 10 GO anthology (Molecular Function) results for upregulated differentially expressed genes in the Cobb 500 and Ross 308 hybrids

Molecular Function in the Cobb 500 breed	Count	-Log <i>P</i> -value
Receptor activity	85	12.96
Molecular transducer activity	85	12.96
Signaling receptor activity	75	12.10
Transmembrane signaling receptor activity	70	12.09
Transmembrane receptor activity	72	12.06
Cytokine receptor activity	19	11.09
Signal transducer activity	83	10.57
Receptor binding	38	5.80
Purinergic receptor activity	9	5.62
G-protein coupled purinergic nucleotide receptor activity	7	5.29
Molecular Function in the Ross 308 breed	Count	-Log <i>P</i> -value
Cytokine receptor activity	19	11.92
Signal transducer activity	79	11.44
Transmembrane signaling receptor activity	62	10.48
Molecular transducer activity	73	10.19
Receptor activity	73	10.19
Transmembrane receptor activity	63	10.09
Signaling receptor activity	64	9.39
Purinergic receptor activity	10	7.21
Nucleotide receptor activity	9	6.66
Purinergic nucleotide receptor activity	9	6.66

days postinfection, viral loads in the Ross tracheal samples were significantly higher than those in the Cobb tracheal samples.

The innate immune response is the first line of defense against pathogens and can be achieved through physical barriers, such as skin and mucous membranes. Other components play non-specific protective roles. These include PRRs, heterophils, macrophages, dendritic cells (DCs), natural killer (NK) cells, acute-phase proteins, the complement system, cytokines, chemokines, and other factors for immune cell trafficking and apoptosis. PRRs of the immune system, such as TLRs, RLRs, and NLRs are involved in early identification of infectious agents [31]. TLRs are key to efficient functioning because they identify protected structures in many pathogens. So far, TLR-1A, TLR-1B, TLR-2A, TLR-2B, TLR-3, TLR-4, TLR-5, TLR-7, TLR-15, and TLR-21 have been identified in chickens [32].

In this study, an increase in expression of the genes encoding TLR-1A, TLR-1B, TLR-2A, TLR-2B, TLR-4, TLR-7, and TLR-15 was found in both hybrids, although their values differed. Unlike the Ross 308 hybrid, the gene encoding TLR-3 exhibited increased expression in the Cobb 500 hybrid. TLR-4 and TLR-15 have been reported to be involved in initiating immune responses to viral infections. Their genes have been shown to undergo increased

expression following infections caused by coronaviruses, including severe acute respiratory syndrome coronavirus (SARS-CoV), IBV, and mouse hepatitis virus (MHV) [33, 34]. Consistent with our study, previous studies have found increased levels of TLR-15 in the lungs of chickens infected with Marek's disease virus (MDV), infectious bursal disease virus (IBDV), and H9N2 influenza viruses [35]. A study conducted by Wang et al. found increased expression of TLR-3 three days after infection with IBV-M41 [14]. TLR-3 has been shown to play an important role in viral immunology [14, 35, 36]. Increased levels of TLR-1A, TLR-1B, TLR-2, TLR-3, and TLR-7 have been found in the epithelial cells of 21-day-old chickens vaccinated with the attenuated IBV vaccine strain Massachusetts [37]. Kameka et al. reported an increase in TLR-3 and TLR-7 levels in tracheal and lung tissues in chickens infected with the Connecticut strain of IBV [38]. Chen et al. reported that TLR-7 mainly recognizes single-stranded RNA (ssRNA) sequences of RNA viruses that enter endosomes by endocytosis [39].

Different pathogen-associated molecular patterns (PAMPs) have been reported to activate different TLRs, inducing production of type I interferons (IFNs). Activation of IFN, in turn, induces expression of interferon-stimulated genes (ISGs) [18, 40]. Although the gene encoding IFN- α in the Cobb 500 hybrid was identified as a DEG in this study,

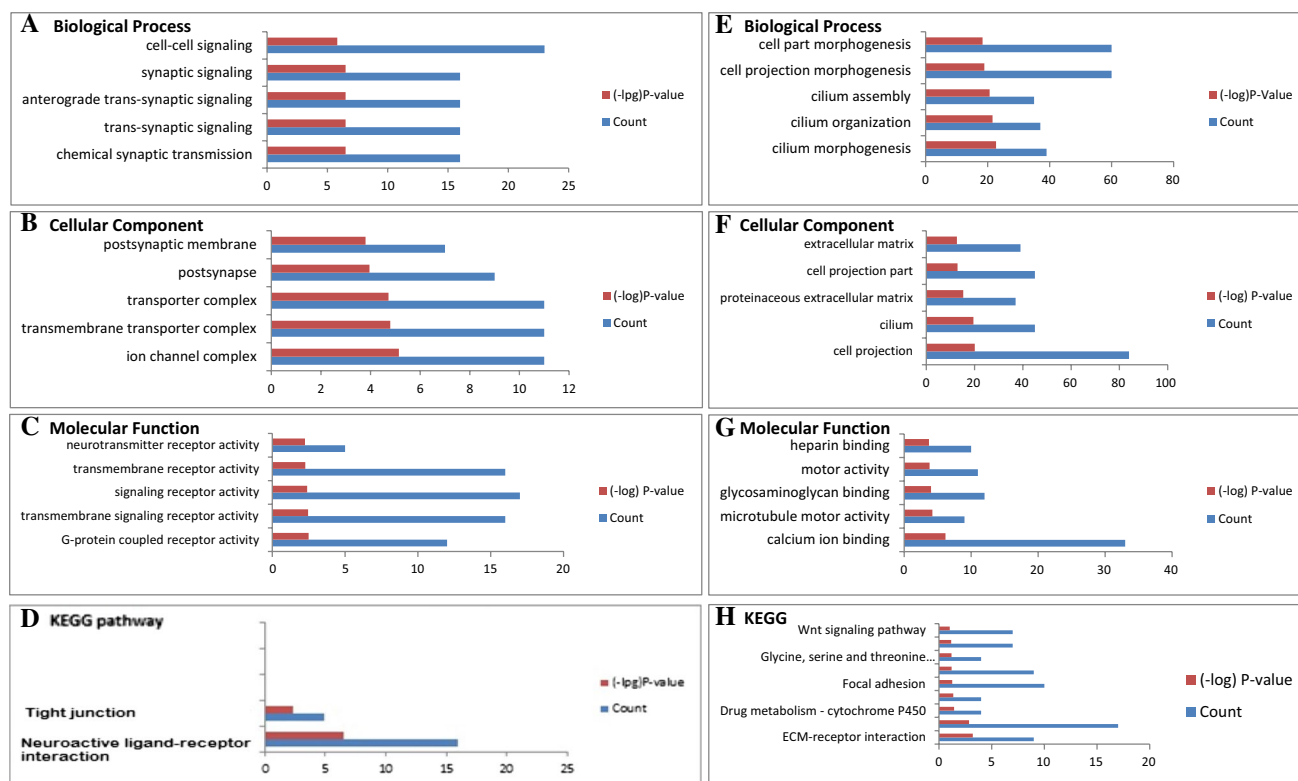


Fig. 4 Comparison of the top five GO ontology (Biological Process, Cellular Component, and Molecular Function) and KEGG pathway results for downregulated differentially expressed genes in the Cobb

500 (A-D) and the Ross 308 hybrids (E-H). "Count" indicates the number of genes involved in each category.

in the Ross 308 hybrid, no increase in the expression of this gene was observed. Also, an increase in the expression of some ISGs and interferon-regulatory factors (IRFs), including IRF4, IRF5, IRF7, IRF8, IRF9, IFIT5, IFITM5, IFIH1, IFI6, IFI30, IFI35, IFI27L2, MYD88, MX1, and RSAD2 was observed in the Cobb 500 hybrid, while increased expression of IRF1, IRF5, IFIT5, IFITM5, IFI6, and IFI30 was observed in the Ross 308 hybrid.

Our results suggest that the induction of IFN- α stimulated stronger expression of ISG and IFI in the Cobb 500 hybrid than in the Ross 308 hybrid. On the other hand, it can be said that IFN- α plays a more important role in stimulating ISGs and IFIs. Furthermore, as mentioned above, the gene encoding TLR-3 exhibited increased expression in the Cobb 500 hybrid after infection. TLR-3, a member of the TLR family of proteins, recognizes viral double-stranded RNA (dsRNA) and induces type I IFN [40]. Since coronaviruses produce dsRNA intermediates during replication [17], the stronger expression of ISG and IFI observed in the Cobb 500 hybrid might be attributed to increased expression of the gene encoding TLR-3.

Phagocytic heterophils and macrophages are among the cells utilized when the innate immune system is activated [31]. It has been reported that heterophils destroy

IBV-infected cells by releasing enzymes [41]. Guo et al. found increased expression of antimicrobial cytotoxic molecules, including bactericidal permeability-increasing protein (BPI) and cathepsin S (CTSS), both of which are released by degranulation of neutrophils [41]. Likewise, in the present study, both hybrids experienced increased expression of CTSS, although to different levels. Several studies have suggested that respiratory macrophages may restrict IBV proliferation in respiratory tissues [38, 41–43].

In line with these findings, an increase in the level of SPI-1 gene expression was observed for both hybrids. Playing a key role in macrophage and monocyte signaling pathways, SPI-1 distinguishes macrophages [44]. Increased expression of the SPI-1 gene was reported in chickens infected with IBV strain Massachusetts [37]. Increased expression was also found for a set of other immune-related genes, including complement system genes encoding C1S, C3, C1R, and C4. These results suggest that both adaptive and innate immunity play a role in the response to IBV, while the complement system acts as a bridge between the innate and adaptive immune responses to provide a comprehensive defense against pathogens [45].

Analysis of the trachea transcriptome revealed that the Cobb 500 hybrid infected with IBV also activated the RLR

Table 7 Comparison of KEGG pathway analysis for upregulated differentially expressed genes in the Cobb 500 and Ross 308 hybrids

KEGG pathway in the Cobb breed	Count	-Log <i>P</i> -value
Cytokine-cytokine receptor interaction	43	19.64
Toll-like receptor signaling pathway	25	11.28
Jak-STAT signaling pathway	26	8.80
Cell adhesion molecules (CAMs)	24	7.85
Influenza A	26	7.77
Intestinal immune network for IgA production	13	7.47
Herpes simplex infection	23	5.17
Phagosome	19	4.00
Cytosolic DNA-sensing pathway	9	2.89
RIG-I-like receptor signaling pathway	10	2.55
NOD-like receptor signaling pathway	8	2.25
Salmonella infection	9	1.55
KEGG pathway in the Ross breed	Count	-Log <i>P</i> -value
Cytokine-cytokine receptor interaction	39	16.89
Cell adhesion molecules (CAMs)	22	6.89
Toll-like receptor signaling pathway	19	6.77
Jak-STAT signaling pathway	22	6.47
Intestinal immune network for IgA production	11	5.66
Phagosome	17	3.26
Herpes simplex infection	18	3.00
NOD-like receptor signaling pathway	8	2.38
Influenza A	15	2.17
Lysosome	13	1.92
Calcium signaling pathway	14	1.11

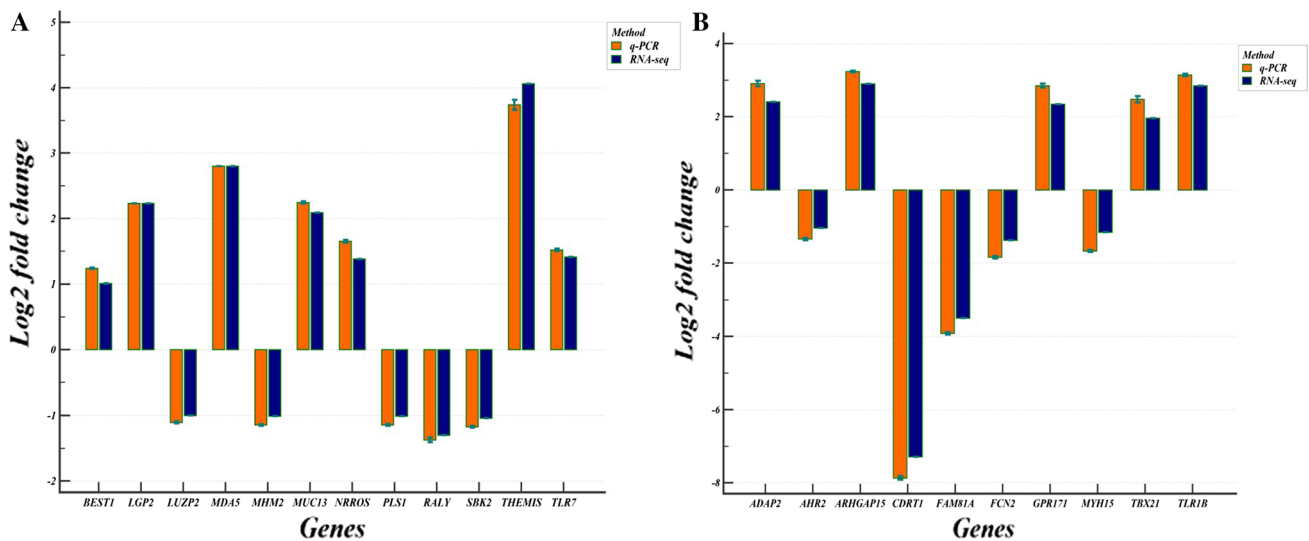


Fig. 5 Comparison of qPCR and RNA-seq quantitation of up- and downregulated genes randomly selected from samples taken from the Cobb 500 (A) and Ross 308 (B) infected groups. The error bars indicate the 95% CI.

Table 8 Expression levels of DEGs selected for RT-qPCR in tracheal samples of the Cobb experimental groups compared to their control groups

Gene	Groups		Statistical analysis
	Cobb experi- mental group-1	Cobb experi- mental group-2	
<i>TLR7</i>	1.52 (0.08)	1.51 (0.07)	$t = 0.45, p = 0.65$
<i>NRROS</i>	1.64 (0.09)	1.65 (0.09)	$t = 0.50, p = 0.62$
<i>THEMIS</i>	3.70 (0.38)	3.77 (0.18)	$t = 0.98, p = 0.33$
<i>BEST1</i>	1.23 (0.05)	1.24 (0.04)	$t = 0.64, p = 0.52$
<i>MUC13</i>	2.24 (0.07)	2.24 (0.08)	$t = 0.18, p = 0.85$
<i>MDA5</i>	2.77 (0.20)	2.80 (0.30)	$t = -0.34, p = 0.73$
<i>LGP2</i>	2.60 (0.33)	2.23 (0.40)	$t = 0.29, p = 0.77$
<i>MHM2</i>	-1.14 (0.04)	-1.15 (0.05)	$t = 0.61, p = 0.55$
<i>LUZP2</i>	-1.10 (0.06)	-1.11 (0.06)	$t = 0.46, p = 0.65$
<i>PLS1</i>	-1.14 (0.05)	-1.15 (0.05)	$t = 0.70, p = 0.48$
<i>RALY</i>	-1.36 (0.13)	-1.38 (0.14)	$t = 0.41, p = 0.68$
<i>SBK2</i>	-1.16 (0.05)	-1.18 (0.05)	$t = 0.95, p = 0.35$

Numbers in parentheses indicate SD

Table 9 Expression levels of DEGs selected for RT-qPCR in tracheal samples of the Ross experimental groups compared to their control groups. Numbers in parentheses indicate SD.

Gene	Groups		Statistical analysis
	Ross experi- mental group-1	Ross experi- mental group-2	
<i>TBX21</i>	2.48 (0.34)	2.47 (0.36)	$t = 0.07, p = 0.94$
<i>TLR1B</i>	3.13 (0.15)	3.16 (0.12)	$t = 0.71, p = 0.48$
<i>GPR171</i>	2.86 (0.21)	2.84 (0.22)	$t = 0.40, p = 0.69$
<i>ADAP2</i>	2.91 (0.30)	2.90 (0.29)	$t = 0.13, p = 0.89$
<i>ARHGAP15</i>	3.25 (0.07)	3.23 (0.10)	$t = 1.01, p = 0.31$
<i>FAM81A</i>	-3.93 (0.13)	-3.90 (0.14)	$t = 0.68, p = 0.50$
<i>AHR2</i>	-1.35 (0.13)	-1.34 (0.13)	$t = 0.06, p = 0.95$
<i>MYH15</i>	-1.68 (0.13)	-1.66 (0.12)	$t = 0.75, p = 0.45$
<i>CDRT1</i>	-7.87 (0.20)	-7.86 (0.19)	$t = 0.26, p = 0.79$
<i>FCN2</i>	-1.84 (0.15)	-1.84 (0.15)	$t = 0.08, p = 0.94$

signaling pathway. RLRs are a group of cytosolic PRRs that trigger an innate antiviral response in infected cells. The RLR group consists of three members: RIG-I, MDA5, and LGP2. Despite the key role of RIG-I in viral infections, its gene has not been identified in chickens [46, 47].

Several studies have suggested that, in the absence of the RIG-I gene in chickens, MDA5 plays a similar role. For instance, it has been reported that influenza A virus (AIV) infection in chicken cells is detected by MDA5 [46]. Although Keestra et al. have suggested that MDA5

compensates for the lack of RIG-I in chickens [48], Barber et al. reported that the absence of RIG-I in chickens negatively affects the antiviral innate immune response induced by the RLR signaling pathway [49]. However, a study by Liniger et al. showed that MDA5 was functionally responsible for sensing AIV in the absence of RIG-I [46].

Yang et al. evaluated gene expression in chicken cells and found that IBV infection induced messenger RNA (mRNA) expression of MDA5 and LGP2 [50]. In this study, we observed an increase in the level of MDA5 and LGP2 gene expression only in the Cobb 500 hybrid. A study by Loo and Gale demonstrated that MDA5 induced the expression of the IRF7 and NF- κ B genes [47]. Consistent with Loo and Gale's study, we observed an increase in the levels of IRF7 and NF- κ B only in the Cobb 500 hybrid.

The Cobb 500 hybrid also showed an increase in the level of TRIM25 gene expression. TRIM25 is a member of the tripartite motif (TRIM) family that regulates the RLR signaling pathway. The TRIM family consists of two members: TRIM25 and TRIM27. Although chickens lack a TRIM27 gene, it has been shown that TRIM25 plays a critical role in inducing antiviral responses in chickens [51]. Xu et al. have suggested that the RLR signaling pathway plays a more important role in the detection of nephropathogenic IBV infection than the TLR signaling pathway [17].

Conclusion

In this study, the Ross 308 and Cobb 500 hybrids exhibited differences in their viral loads and transcriptome profiles in tracheal tissues two days after infection with IBV. Viral loads in tracheal samples from the Ross challenged group were significantly higher than those in the Cobb challenged group. Furthermore, a larger number of downregulated genes were identified in the Ross 308 hybrid two days after IBV infection. The trachea transcriptome analysis also revealed that, unlike the Ross 308 hybrid, increased expression of TLR-3, chicken interferon α (ChIFN- α), and other components involved in the RLR signaling pathway such as MDA5, LGP2, IRF-7, NF- κ B, and TRIM25 were observed for the Cobb 500 line. TLR-3 has been reported to play an important role in the antiviral response and to induce ChIFN- α [35, 36, 40]. Furthermore, a previous study has suggested that ChIFN- α inhibits IBV replication and is associated with respiratory illness [1]. In addition, the role of the RLR signaling pathway in the innate antiviral response should not be ignored.

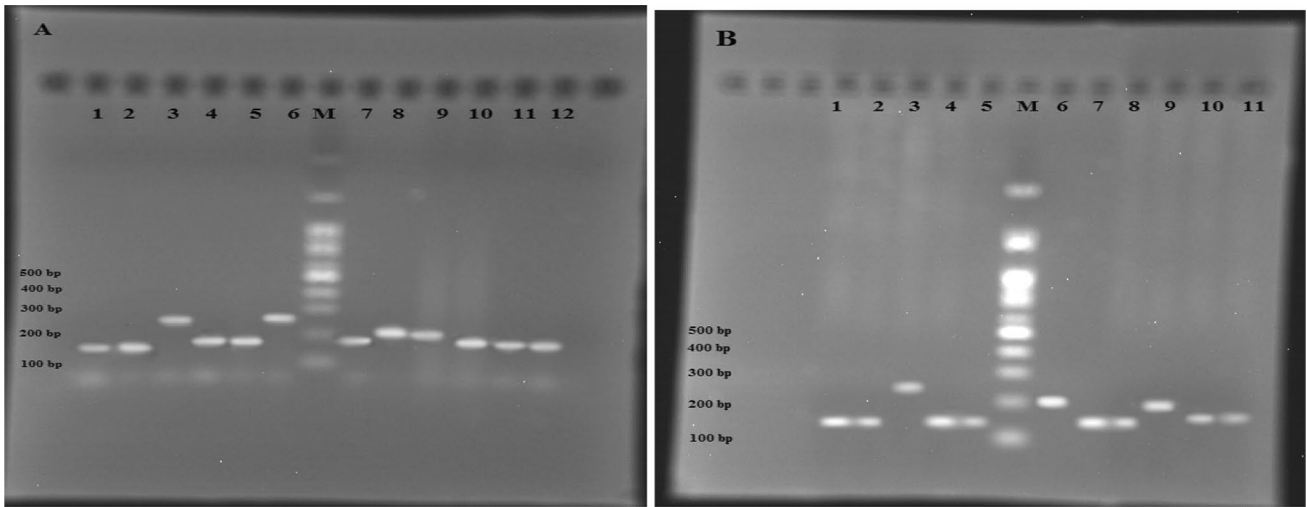


Fig. 6 Agarose gel electrophoresis results of DEGs selected for RT-qPCR assay. (A) Cobb. 1, *PALY* (155 base pair [bp]); 2, *PLS1* (158 bp); 3, *THEMIS* (239 bp); 4, *BEST1* (172 bp); 5, *MUC13* (172 bp); 6, *MDA5* (244 bp); 7, *LGP2* (193 bp); 8, *SBK2* (214 bp); 9, *MHM2* (217 bp); 10, *TLR1B* (173 bp); 11, *LUZP2* (169 bp); 12, *NRROS* (163

bp). (B) Ross. 1, *MYH15* (163 bp); 2, *TBX21* (162 bp); 3, *ADAP2* (239 bp); 4, *GAPDH* (162 bp); 5, *AHR2* (153 bp); 6, *GPR171* (204 bp); 7, *TLR1B* (173 bp); 8, *CDRT1* (175 bp); 9, *FCN2* (203 bp); 10, *FAM81A* (188 bp); 11, *ARHGAP15* (182 bp). M, 100 bp marker

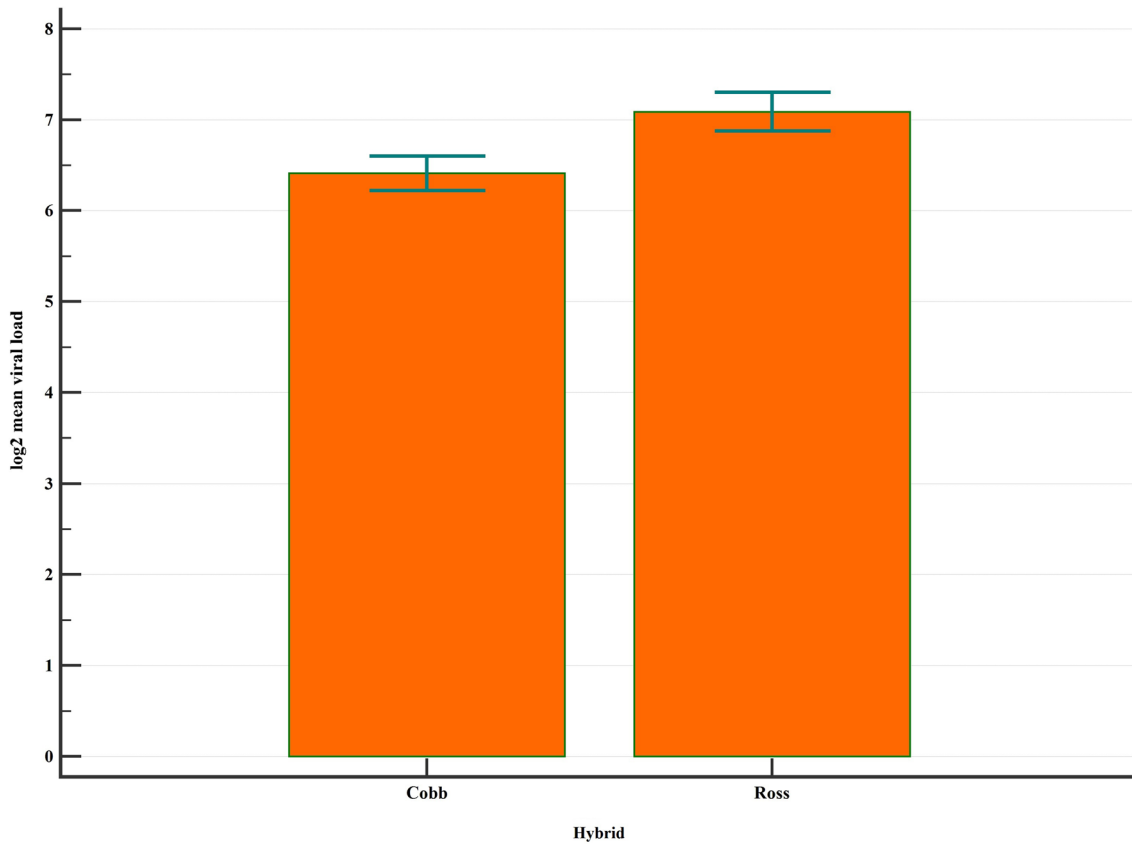


Fig. 7 Comparison of log₂ mean viral loads in samples from challenged groups. The error bars indicate the 95% CI of the mean; $P < 0.0001$.

It appears likely that the Cobb 500 hybrid exerts a more robust immune response to IBV infection than the Ross 308 hybrid. Furthermore, the results of this study suggest that increased expression of TLR-3, ChIFN- α , and other components involved in the RLR signaling pathway (such as MDA5, LGP2, IRF-7, NF- κ B, and TRIM25) may interfere with IBV proliferation. This could be considered a potential area for future research.

Supplementary Information The online version contains supplementary material available at <https://doi.org/10.1007/s00705-021-05322-5>.

Acknowledgements The authors gratefully acknowledge the Sheikh Bahaei National High-Performance Computing Center (SBNHPCC) for providing computing facilities and time. SBNHPCC is supported by the Presidential Office's Scientific and Technological Department and Isfahan University of Technology.

References

- Barjesteh N, O'Dowd K, Vahedi SM (2020) Antiviral responses against chicken respiratory infections: focus on avian influenza virus and infectious bronchitis virus. *Cytokine* 127:154961
- Nawab A et al (2019) Chicken toll-like receptors and their significance in immune response and disease resistance. *Int Rev Immunol* 38(6):284–306
- Liu H et al (2017) Comparative transcriptome analysis reveals induction of apoptosis in chicken kidney cells associated with the virulence of nephropathogenic infectious bronchitis virus. *Microb Pathog* 113:451–459
- Reddy VR et al (2015) Genetic characterization of the Belgian nephropathogenic infectious bronchitis virus (NIBV) reference strain B1648. *Viruses* 7(8):4488–4506
- Jackwood MW, Hall D, Handel A (2012) Molecular evolution and emergence of avian gammacoronaviruses. *Infect Genet Evol* 12(6):1305–1311
- Ambali A, Jones R (1990) Early pathogenesis in chicks of infection with an enterotropic strain of infectious bronchitis virus. *Avian Dis* 34:809–817
- Awad F et al (2014) An overview of infectious bronchitis virus in chickens. *Worlds Poult Sci J* 70(2):375–384
- Benyeda Z et al (2009) Comparison of the pathogenicity of QX-like, M41 and 793/B infectious bronchitis strains from different pathological conditions. *Avian Pathol* 38(6):449–456
- De Wit J et al (2011) Induction of cystic oviducts and protection against early challenge with infectious bronchitis virus serotype D388 (genotype QX) by maternally derived antibodies and by early vaccination. *Avian Pathol* 40(5):463–471
- Ganapathy K et al (2012) QX-like infectious bronchitis virus isolated from cases of proventriculitis in commercial broilers in England. *Vet Rec* 171(23):597
- Jackwood MW, De Wit S (2013) Infectious bronchitis. *Dis Poultry*. <https://doi.org/10.1002/9781119421481.ch4>
- Raj GD, Jones R (1997) Infectious bronchitis virus: immunopathogenesis of infection in the chicken. *Avian Pathol* 26(4):677–706
- Hamzić E et al (2016) RNA sequencing-based analysis of the spleen transcriptome following infectious bronchitis virus infection of chickens selected for different mannose-binding lectin serum concentrations. *BMC Genomics* 17(1):1–13
- Wang X et al (2006) Transcriptome of local innate and adaptive immunity during early phase of infectious bronchitis viral infection. *Viral Immunol* 19(4):768–774
- Jordan B (2017) Vaccination against infectious bronchitis virus: a continuous challenge. *Vet Microbiol* 206:137–143
- Meir R et al (2012) Immune responses to mucosal vaccination by the recombinant S1 and N proteins of infectious bronchitis virus. *Viral Immunol* 25(1):55–62
- Xu P et al (2019) A Multi-omics study of chicken infected by nephropathogenic infectious bronchitis virus. *Viruses* 11(11):1070
- Cong F et al (2013) Transcriptome analysis of chicken kidney tissues following coronavirus avian infectious bronchitis virus infection. *BMC Genomics* 14(1):1–13
- Lin X et al (2015) Insights into human astrocyte response to H5N1 infection by microarray analysis. *Viruses* 7(5):2618–2640
- Najafi H et al (2016) Pathogenicity characteristics of an Iranian variant-2 (IS-1494) like infectious bronchitis virus in experimentally infected SPF chickens. *Acta Virol* 60(4):393–399
- Ren G et al (2020) Pathogenicity of a QX-like avian infectious bronchitis virus isolated in China. *Poult Sci* 99(1):111–118
- Rauw W et al (1998) Undesirable side effects of selection for high production efficiency in farm animals: a review. *Livest Prod Sci* 56(1):15–33
- Najafi H et al (2016) Molecular characterization of infectious bronchitis viruses isolated from broiler chicken farms in Iran, 2014–2015. *Adv Virol* 161(1):53–62
- Reed LJ, Muench H (1938) A simple method of estimating fifty per cent endpoints. *Am J Epidemiol* 27(3):493–497
- Dobin A et al (2013) STAR: ultrafast universal RNA-seq aligner. *Bioinformatics* 29(1):15–21
- Huang DW, Sherman BT, Lempicki RA (2009) Bioinformatics enrichment tools: paths toward the comprehensive functional analysis of large gene lists. *Nucleic Acids Res* 37(1):1–13
- Ye J et al (2012) Primer-BLAST: a tool to design target-specific primers for polymerase chain reaction. *BMC Bioinformatics* 13(1):1–11
- Livak KJ, Schmittgen TD (2001) Analysis of relative gene expression data using real-time qPCR and the 2⁻ $\Delta\Delta$ CT method. *Methods* 25(4):402–408
- Abdollahi H et al (2021) Coronavirus: proteomics analysis of chicken kidney tissue infected with variant 2 (IS-1494)-like avian infectious bronchitis virus. *Adv Virol* 166(1):101–113
- Kanehisa M et al (2019) New approach for understanding genome variations in KEGG. *Nucleic Acids Res* 47(D1):D590–D595
- Chhabra R, Chantrey J, Ganapathy K (2015) Immune responses to virulent and vaccine strains of infectious bronchitis viruses in chickens. *Viral Immunol* 28(9):478–488
- Paul MS et al (2013) Immunostimulatory properties of Toll-like receptor ligands in chickens. *Vet Immunol Immunopathol* 152(3–4):191–199
- Bowie AG, Haga IR (2005) The role of Toll-like receptors in the host response to viruses. *Mol Immunol* 42(8):859–867
- Okabayashi T et al (2006) Cytokine regulation in SARS coronavirus infection compared to other respiratory virus infections. *J Med Virol* 78(4):417–424
- Le Goffic R et al (2007) Cutting Edge: Influenza A virus activates TLR3-dependent inflammatory and RIG-I-dependent antiviral responses in human lung epithelial cells. *J Immunol* 178(6):3368–3372
- Liu P et al (2007) Retinoic acid-inducible gene I mediates early antiviral response and Toll-like receptor 3 expression in respiratory syncytial virus-infected airway epithelial cells. *J Virol* 81(3):1401–1411

37. Guo X et al (2008) Molecular mechanisms of primary and secondary mucosal immunity using avian infectious bronchitis virus as a model system. *Vet Immunol Immunopathol* 121(3–4):332–343
38. Kameka AM et al (2014) Induction of innate immune response following infectious bronchitis corona virus infection in the respiratory tract of chickens. *Virology* 450:114–121
39. Chen S, Cheng A, Wang M (2013) Innate sensing of viruses by pattern recognition receptors in birds. *Vet Res* 44(1):1–12
40. Matsumoto M, Seya T (2008) TLR3: interferon induction by double-stranded RNA including poly (I: C). *Adv Drug Deliv Rev* 60(7):805–812
41. Fulton R et al (1997) Effect of Cytoxan®-induced heteropenia on the response of specific-pathogen-free chickens to infectious bronchitis. *Avian Dis* 41:511–518
42. Dar A et al (2005) Transcriptional analysis of avian embryonic tissues following infection with avian infectious bronchitis virus. *Virus Res* 110(1–2):41–55
43. Matthijs MG et al (2009) Course of infection and immune responses in the respiratory tract of IBV infected broilers after superinfection with *E. coli*. *Vet Immunol Immunopathol* 127(1–2):77–84
44. Garceau V et al (2010) Pivotal Advance: Avian colony-stimulating factor 1 (CSF-1), interleukin-34 (IL-34), and CSF-1 receptor genes and gene products. *J Leukoc Biol* 87(5):753–764
45. Dunkelberger JR, Song W-C (2010) Complement and its role in innate and adaptive immune responses. *Cell Res* 20(1):34–50
46. Liniger M et al (2012) Chicken cells sense influenza A virus infection through MDA5 and CARDIF signaling involving LGP2. *J Virol* 86(2):705–717
47. Loo Y-M, Gale M Jr (2011) Immune signaling by RIG-I-like receptors. *Immunity* 34(5):680–692
48. Keestra AM et al (2013) Unique features of chicken Toll-like receptors. *Dev Comp Immunol* 41(3):316–323
49. Barber MR et al (2010) Association of RIG-I with innate immunity of ducks to influenza. *Proc Natl Acad Sci* 107(13):5913–5918
50. Yang X et al (2018) Induction of innate immune response following introduction of infectious bronchitis virus (IBV) in the trachea and renal tissues of chickens. *Microb Pathog* 116:54–61
51. Rajsbaum R et al (2012) Species-specific inhibition of RIG-I ubiquitination and IFN induction by the influenza A virus NS1 protein. *PLoS Pathog* 8(11):e1003059

Publisher's Note Springer Nature remains neutral with regard to jurisdictional claims in published maps and institutional affiliations.